Beta Decay of N^{16} to the 6.05-MeV State of O^{16}†

E. K. WARBURTON, W. R. HARRIS, AND D. E. ALBURGER
Brookhaven National Laboratory, Upton, New York 11973
(Received 14 June 1968)

The β-ray branching of N^{16} to the 6.05-MeV 0^+ first excited state of O^{16} has been detected by observing the subsequent positron-electron nuclear pair emission from the 6.05-MeV level with a magnetic pair spectrometer. A previously developed spiral baffle system was used in the spectrometer to enhance the sensitivity for detecting the 6.05-MeV $E0$ pair line relative to the 6.13-MeV $E3$ pair line, the latter following the principal N^{16} β-ray branch. The branch to the 6.05-MeV state was found to be $(1.2\pm0.4)\times10^{-4}$ per decay. Based on the measured branching ratios, the $\log f_1 t$ values for the unique first-forbidden decays to the ground and 6.05-MeV states are calculated to be 9.12 ± 0.04 and 9.98 ± 0.15, respectively. The results are consistent with recent descriptions of the ground and first excited states of O^{16}.

INTRODUCTION

NITROGEN–16 decays by β-ray emission with a half-life of 7.37 sec and a total decay energy of 10.42 MeV. In a previous study[1] of the β decay of N^{16} an attempt was made to observe a β-ray branch to the 6.05-MeV 0^+ first excited state of O^{16}. Since N^{16} has a spin parity of 2^- the sought-for branch is unique first forbidden, as is the known 26% branch to the 0^+ ground state. The principal β-ray decay of N^{16} is the allowed transition to the 6.13-MeV 3^- state of O^{16} which is a 68% branch having $\log f_0 t = 4.5$. Several weaker branches are also present leading to higher levels of O^{16}.

The method used in the earlier work[1] was to measure the positron-electron pair coincidence spectrum of N^{16} by means of an intermediate-image pair spectrometer.[2] The dominant feature of this spectrum is the pair line associated with the 6.13-MeV $E3$ transition following the β-ray feeding of this level. Because the internal-pair conversion probability is only 1.48×10^{-3} for an $E3$ transition of 6.13 MeV as compared with nearly unity for an $E0$ transition of 6.05 MeV it was hoped that even a very weak β-ray branch to the 6.05-MeV level could be detected by observing the corresponding pair coincidence line. A spectrometer resolution setting of $\sim1.3\%$ was used since the 6.05- and 6.13-MeV pair lines differ in momentum by only 1.34%. In that experiment the 6.05-MeV pair line was not observed and an upper limit of 10% was placed on its amplitude relative to the amplitude of the 6.13-MeV pair line. By making use of the relative over-all spectrometer efficiencies for detecting $E3$ and $E0$ electromagnetic transitions at 6 MeV ($\epsilon_{E0}/\epsilon_{E3}=462$), together with the known β-ray branch to the 6.13-MeV state, the result corresponds to an upper limit of $<1.5\times10^{-4}$ on the β-ray branching of N^{16} to the 6.05-MeV state. A lower limit of 8.2 was placed on the corresponding $\log f_0 t$ value. These earlier calculations of the $\log ft$ values for the decays to both the ground and first excited states made use of the Fermi function f_0 appropriate to allowed β-ray transitions rather than the function f_1 which is proper for unique first-forbidden decays. This is discussed below.

During the intervening years since the above measurements were made on N^{16} the concept of using the intermediate-image pair spectrometer to determine the multipolarities of electromagnetic transitions was proposed and the technique developed.[3–5] The method incorporates a spiral baffle system of special design which essentially allows one to make a two-point angular correlation measurement of the positron-electron internal-pair conversion electrons. A pair coincidence line is measured first without the baffle and then with the baffle inserted in the paths of the focused electrons. Information on the multipolarity of the transition is derived from the measured value of R_ω which is the ratio of the amplitudes of the line with the baffle "in" to the line with the baffle "out."

For the purposes of the present paper we need consider only the values of R_ω for the 6.13-MeV $E3$ transition and for the 6.05-MeV $E0$ transition. According to the spectrometer calibration data[4] the value of R_ω for the $E3$ transition is 0.051, whereas for the $E0$ transition it is 0.256. Although the spiral baffle reduces the intensities of both lines its use evidently results in a relative enhancement of the $E0$ line by a factor of 5.0, i.e., the ratio of $E0/E3$ spectrometer efficiencies for detecting these transitions is predicted to be 2320 with the baffle in place. By taking advantage of this further discrimination in favor of the $E0$ transition we have been able to detect a very weak N^{16} β-ray branch to the 6.05-MeV state of O^{16}.

EXPERIMENTAL METHODS

In many respects this new experiment was similar to the earlier study[1] of N^{16}, the main difference being that this time the pair-line spectrum was measured with the spiral baffle inserted. Several other significant improvements were also made in the general method. N^{16}

† Work performed under the auspices of the U. S. Atomic Energy Commission.

[1] D. E. Alburger, Phys. Rev. **111**, 1586 (1958).

[2] D. E. Alburger, Rev. Sci. Instr. **27**, 991 (1956).

[3] E. K. Warburton, D. E. Alburger, A. Gallmann, P. Wagner, and L. F. Chase, Jr., Phys. Rev. **133**, B42 (1964).

[4] J. W. Olness, E. K. Warburton, D. E. Alburger, and J. A. Becker, Phys. Rev. **139**, B512 (1965).

[5] E. K. Warburton and D. E. Alburger, in *Nuclear Spin-Parity Assignments*, edited by N. B. Gove and R. L. Robinson (Academic Press Inc., New York, 1966), p. 114.

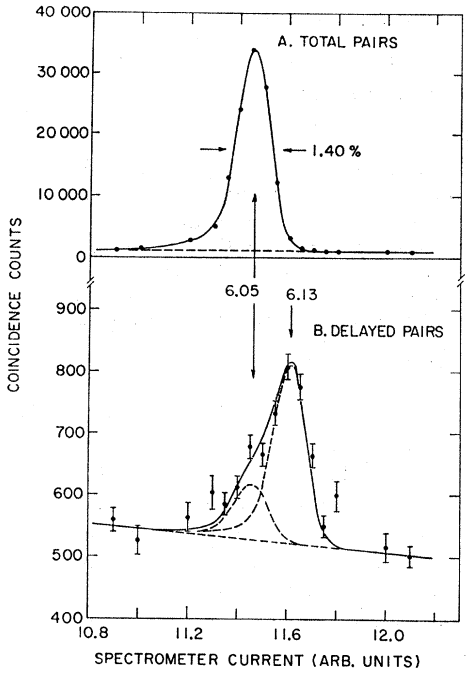

FIG. 1. Pair-line spectra from $N^{15}+d$ at $E_d=2.8$ MeV measured in the intermediate-image spectrometer with the spiral baffle inserted. Total data accumulation time was 460 h. (A) total pairs resulting almost entirely from direct population of the 6.05-MeV state in the $N^{15}(d,n)O^{16}$ reaction. (B) delayed pairs occurring in the β decay of N^{16}. The line corresponding to the weak branch to the 6.05-MeV level is evident in the N^{16} spectrum as is the 6.13-MeV line from the main β-decay mode.

activity was again formed via the $N^{15}(d,p)N^{16}$ reaction using a TiN^{15} target several mg/cm^2 thick; but instead of the previous method of 7-sec bombardment and 7-sec count intervals a fast mechanical beam chopper was used.[6] Aside from producing a nearly constant equilibrium activity of N^{16} because of the short cycle of irradiation and counting (3-msec irradiation, 1-msec delay, 12 msec of counting, and 1-msec delay) the counting time with this device is 70% of the total time. These features result in a higher average real counting rate for a given random coincidence rate.

A distinct advantage arose in the use of the fast beam chopper which was not anticipated when the measurements were planned. During the 3-msec target bombardment portion of the irradiate-count cycle the competing reaction $N^{15}(d,n)O^{16}$ forms the states of O^{16} directly. Just as in the case of the reaction $F^{19}(p,\alpha)O^{16}$, which is used routinely for pair spectrometer calibration purposes, the 6.05-MeV $E0$ pair line from $N^{15}(d,n)O^{16}$ completely dominates the pair-line spectrum from $N^{15}+d$ reactions. Thus by counting *all* pairs from the detector the 6.05-MeV line is recorded with high statistical accuracy. The 6.05-MeV level is sufficiently long lived so that the pair line in the prompt reaction does not suffer Doppler effects; hence this line can serve as a precise calibration reference for both position and experimental line shape, as well as providing a continuous check on yield and on the over-all stability of the spectrometer current control. Evidently the 6.05-MeV prompt line will give the desired shape of a single line for computer fitting of the N^{16} pair-line spectrum that occurs during the 12-msec delayed counting interval. The latter counts are selected by means of a gating circuit.

There is a danger in applying the beam-chopper technique to the present problem, where the sought-for line in the delayed spectrum is the very same one that occurs with a relatively large intensity in the prompt spectrum—and that danger is the possibility of either beam leak-through or electronic leak-through. Even a very small amount of stray beam striking the target during the delayed or "beam-off" portion of the cycle would result in the appearance of a delayed 6.05-MeV line. To be more certain of counteracting beam leak-through an antiscattering baffle had been inserted close to the beam-chopping cylinder prior to the runs on N^{16}. Electronic leak-through was thought to be very unlikely since no such effects have ever been observed when using the beam-chopper system even in very sensitive experiments.

As an experimental test for all types of leak-through effects a CaF_2 target was placed in the spectrometer and the 6.05-MeV state of O^{16} was formed via the $F^{19}(p,\alpha)O^{16}$ reaction. With the beam chopper operating in exactly the same way as in the N^{16} experiment, and with the spectrometer baffles set for maximum transmission, the spectrometer current was adjusted to focus the peak of the 6.05-MeV pair line. In two such test runs of 1 h each, one made in conjunction with each of the long N^{16} runs to be described below, a total of 2×10^5 prompt pair counts were recorded. During this same period only two counts (of undetermined origin) occurred in the delayed spectrum. It was concluded that leak-through effects were completely negligible since at most they could account for only a few percent of the 6.05-MeV pair line observed in the N^{16} delayed spectrum discussed below.

Other details of the spectrometer operation were the same as in the earlier work. In particular the spectrometer was set for the same momentum resolution ($\sim$1.4%) and the resolving time of the coincidence circuit was 1 nsec.

EXPERIMENTAL RESULTS AND ANALYSIS

Two runs were made on the N^{16} pair-line spectrum. In both cases the deuteron beam had an energy of 2.8 MeV and an average current of 0.1 μA on the target; data accumulation times were 240 and 220 h for the first and second runs, respectively. Prior to the second run a further improvement in technique was to install spectrostats for supplying the high voltage to the photomultipliers used in the pair detector. These devices stabilized the over-all gains so as to maintain the pulse-height peaks, due to focused electrons, centered in the

[6] D. E. Alburger, Phys. Rev. 131, 1624 (1963).

fixed pulse-height windows of the coincidence circuit. The stabilizers operated at a mean output voltage of 1850 V and they did not require manual adjustments over the range of the spectrometer settings selected. In order to minimize possible systematic errors the sequence of points in this run was randomized.

Although several of the spectrometer settings used in the second run were different from those of the first run it was still possible to combine the two runs after making a small normalization correction. Figure 1B shows the combined spectrum of delayed pairs due to N^{16} and Fig. 1A shows the combined spectrum of *all* pairs. As explained previously, the latter spectrum results from the prompt formation of the 6.05-MeV level in the $N^{15}(d,n)O^{16}$ reaction. It is clear from inspection that the delayed spectrum must contain a 6.05-MeV component in addition to the predominant 6.13-MeV line. About $\frac{1}{3}$ of the background in Fig. 1B is due to random coincidences, while the remainder results from the real coincidences between the continuum of β rays feeding the 6.13-MeV state and the continuum of positrons from the internal-pair conversion of the 6.13-MeV transition.

In order to analyze the delayed spectrum a fit to the prompt curve of Fig. 1A was first made so as to establish the line-shape response of the spectrometer and the position of the 6.05-MeV line. The line-shape response function used was that of a Gaussian plus an exponential tail[7]: Explicitly, in the absence of background, a single line positioned at a momentum p_0 was assumed to have the form

$$Y(p)=\frac{A}{(2\pi)^{1/2}\sigma}e^{-\frac{1}{2}(\zeta^2/\sigma^2)}+CAe^{-D\zeta}(1-e^{-\frac{1}{2}(\zeta G)^2}), \quad (1)$$

where $\zeta=p-p_0$. The parameters σ, C, D, and G describe the spectrometer line shape and were assumed to be independent of p_0 in the range of p considered. These parameters, as well as the position (p_0) of the 6.05-MeV peak were determined by the computer fit to the prompt peak shown in Fig. 1A. In this fit the background was included in and determined by the least-squares fit by adding a term $He^{-F\zeta}$ to Eq. (1).

The least-squares fit to the delayed spectrum of Fig. 1B was made with the background fixed by a preliminary least-squares fit to the wings (two extreme points on each side) of the spectrum using $He^{-F\zeta}$. The assumption of an exponential background having the slope given by the computer fitting in Fig. 1B is consistent with the shape of the singles spectrum over the same region as measured in a separate short run. An energy separation of 79 keV between the 6.05- and 6.13-MeV transitions was used in order to calculate the expected spectrometer momentum position of the 6.13-MeV line. This energy difference was derived from the work of Browne and Michael,[8] who give the values 6052±5 keV and 6131±4 keV for the O^{16} levels in question. They do not quote the error on the energy difference, but it is probably not more than ±2 keV. This error would have a negligible effect on the error of the fitting. Thus, under the assumption that only the two expected pair lines of identical shape are present in the N^{16} delayed spectrum with predetermined positions and superimposed on a predetermined background, the only unknowns in the computer fitting of the spectrum are the intensities of the two peaks. In the first run the reliability of the data was brought into question since we were unable to fit the delayed spectrum, given the pair line shape and the positions of the two peaks, to the accuracy implied by the statistical uncertainty of the data ($\chi^2=2.4$). This suggested the possibility of a systematic error and necessitated the second run.

The solid line in Fig. 1B is the computer fit to the combined data of both runs and the dashed peaks show the fits to the two separate pair lines. A peak intensity ratio of 0.32±0.06 ($\chi^2=1.77$) for the 6.05-MeV peak relative to the 6.13-MeV peak results from this fit. Similar analyses of the data of the separate long runs gave 0.262±0.095 ($\chi^2=2.4$) and 0.369±0.052 ($\chi^2=0.5$) for the first and second runs, respectively. The uncertainty associated with the former figure reflects the relatively poor fit to the data of the first run—as mentioned previously. One of the data points that was particularly suspicious in that run was the high point at the spectrometer current setting of 11.8 in Fig. 1B. This particular setting was not used in the second run. In any case the separate results on the intensity ratio agree within their errors.

A fit to the delayed spectrum was also made with the intensity of the 6.05-MeV peak fixed at zero. The result was a 6.13-MeV peak with an intensity 10% greater than that shown by the dashed line of Fig. 1B and a χ^2 of 5.07. As mentioned above, the fit in Fig. 1B has a χ^2 of 1.77 and hence the obvious need for a 6.05-MeV contribution is made quantitative.

Because the background was predetermined in the above fitting procedure, the error given by the computer does not include the error in the background. The latter is parameterized by an error ΔH in the background level, $He^{-F\zeta}$. The error in the peak intensity ratio from this source was estimated by fixing the background level alternately at $H+\Delta H$ and $H-\Delta H$ and repeating the fit to the two peaks. The resulting spread in the peak intensity ratio was taken as an indication of its uncertainty due to uncertainty in the background and was added quadratically to the uncertainty from the first computer fit. The final result is then 0.32±0.10 for the ratio of the 6.05- to 6.13-MeV peak intensities.

Because of the relatively high statistical accuracy of the 6.13-MeV peak amplitude in these "baffle-in" runs it was decided to interrupt the first run half-way through and to measure the 6.13-MeV line with the baffle out in order to derive a value of R_ω for an $E3$ line. In earlier work[3] on N^{16} decay, carried out at the maxi-

[7] E. K. Warburton, J. W. Olness, D. E. Alburger, D. J. Bredin, and L. F. Chase, Jr., Phys. Rev. **134**, B338 (1964).
[8] C. P. Browne and I. Michael, Phys. Rev. **134**, B133 (1964).

TABLE I. Comparison of the γ decay of the O^{16} 13.09-MeV 1^- level and the β decay of N^{16} to the predictions of various nuclear models.

$T=1$ 1p-1h wave functions	$\Lambda(E1)_{g.s.}$	$\frac{\Lambda(E1)_{6.05}}{\Lambda(E1)_{g.s.}}$	$\langle G_1\rangle^2$	$\frac{\langle G_1\rangle_{6.05}^2}{\langle G_1\rangle_{g.s.}^2}$
		$\Psi(O_{g.s.}^{16})=\Psi(s^4p^{12})$		
jj[a]	1.25	0.00	4.52	0.00
EF[b]	0.39	0.00	2.56	0.00
GJ[c]	0.70	0.00	2.70	0.00
KLS[d]	0.37	0.00	1.79	0.00
Brown-Green[e] O^{16} wave functions; 1p-1h $\rightarrow$ 2p-2h=0				
jj	0.95	0.09	3.45	0.09
EF	0.30	0.09	1.96	0.09
GJ	0.53	0.09	2.06	0.09
KLS	0.28	0.09	1.37	0.09
Zuker-Buck-McGrory[f] O^{16} wave functions; 1p-1h $\rightarrow$ 2p-2h estimated				
jj	0.76	0.10	2.02	0.25
EF	0.27	0.05	1.10	0.26
GJ	0.45	0.08	1.16	0.25
KLS	0.26	0.04	0.75	0.26
Expt.	0.63[g]	0.043±0.007[h]	1.49±0.12[i]	0.14±0.05[i]

[a] $p_{1/2}^{-1}d_{5/2}$ and $p_{1/2}^{-1}2s_{1/2}$ for $J_i^\pi=2^-$ and 1^-, respectively.
[b] J. P. Elliott and B. H. Flowers, Proc. Phys. Soc. (London) **A242**, 57 (1957).
[c] V. Gillet and D. A. Jenkins, Phys. Rev. **140**, B36 (1965).
[d] S. Kahana, H. C. Lee, and C. K. Scott (private communication).
[e] Reference 15.
[f] Reference 19.
[g] D. F. Hebbard, Nucl. Phys. **15**, 289 (1960). No errors given, isospin impurity neglected.
[h] Average of values given by S. Gorodetzky, W. Benenson, P. Chevallier, D. Disdier, and F. Scheibling, Phys. Letters **6**, 269 (1963) and Ref. 11.
[i] From present work.

mum spectrometer transmission, an R_ω value of $0.055_{-0.013}^{+0.008}$ was obtained for the 6.13-MeV transition. A larger error was assigned on the low side because of uncertainty as to the possible presence of an unresolved 6.05-MeV component. In the present work the resolution was good enough so that there could be only a few percent contribution at the 6.13-MeV peak due to the 6.05-MeV peak. The result of the measurement was $R_\omega=0.062\pm0.007$ for the 6.13-MeV $E3$ line. This is outside the error when compared with the expected value of 0.051 from previous calibration curves. The very probable reason for the high value of R_ω was discovered after all of the measurements had been completed when it was found the pair detector had inadvertently been moved slightly away from its proper axially centered position. This misalignment had unfortunately gone unnoticed until calibration checks were made on some lines that had been measured previously with high accuracy.

Although the effect of the detector misalignment was less than the error on the final result, it was felt that in the analysis the actual measured value of R_ω should be used for the 6.13-MeV line. Also, prior to realigning the detector the ratio R_ω for the 6.05-MeV line was measured, by using the $F^{19}(p,\alpha)O^{16}$ reaction, and found to be 0.249 ± 0.003. This result also differed from the correct calibration value ($R_\omega=0.256$) but the difference was only a few percent. This was in agreement with our expectations that the value of R_ω for an $E0$ line should be less sensitive to detector misalignment than the value for an $E3$ line.

The observed intensity ratio of the 6.05- and 6.13-MeV pair lines in Fig. 1B may be used, together with the ratio of spectrometer pair-line efficiencies for detecting these two transitions, to derive the transition intensity ratio. Instead of using the previously quoted efficiency ratio $\epsilon_{E0}/\epsilon_{E3}=2320$ based on calibration values established in earlier work, we used the ratio 1850 ± 210 which was derived from the R_ω values actually measured with the detector in the misaligned position. The final result for the ratio of transition intensities is $6.05/6.13=(1.73\pm0.57)\times10^{-4}$.

The observation of a 6.05-MeV pair line in the decay of N^{16} can be ascribed to direct β-ray branching to the 6.05-MeV state or to γ-ray transitions from higher states that are themselves fed by β-ray branches. Consideration of the known β-ray branches of N^{16} to states[1,9] of O^{16} and the γ-ray branches[10–12] from them leads to the conclusion that, with the possible exception of a contribution from the O^{16} $8.88\rightarrow6.05$ γ-ray transition, such feeding is wholly negligible. There has been a report[12] of a measurement of the O^{16} $8.88\rightarrow6.05$ transition giving its intensity relative to the intensity of the $8.88\rightarrow0$ transition as $(1.20\pm0.36)\times10^{-2}$. Previous results on the branching of the 8.88-MeV state to the ground state $(7.2\pm0.8\%)$[11] and on the β-ray branch of N^{16} to the 8.88-MeV state (1.1%),[9] when combined with the result[12] on the $8.88\rightarrow6.05$ transition, would correspond to 9.5×10^{-6} transitions of 6.05 MeV per N^{16} decay. This would represent a contribution to the 6.05-MeV pair line amounting to about 10% of the intensity of the line that we have observed. As can be inferred from later discussion the reported[12] $8.88\rightarrow6.05$ branching intensity is $\gtrsim20$ times stronger than expected. Until the $8.88\rightarrow6.05$ branch is confirmed we believe that our result should not be altered but should be subject to a possible 10% correction. By attributing the 6.05-MeV pair line observed in our work entirely to direct β decay the measured 6.05/6.13 transition ratio given above, together with the known 68% branching to the 6.13-MeV state, may be used to arrive at a final value of $(1.2\pm0.4)\times10^{-4}$ for the β-ray branch of N^{16} to the 6.05-MeV state of O^{16}.

DISCUSSION

The motive for the present experiment was to provide another experimental test for nuclear wave functions

[9] D. H. Wilkinson, B. J. Toppel, and D. E. Alburger, Phys. Rev. **101**, 673 (1956).
[10] J. Lowe, D. E. Alburger, and D. H. Wilkinson, Phys. Rev. **163**, 1060 (1967).
[11] D. H. Wilkinson, D. E. Alburger, and J. Lowe, Phys. Rev. **173**, 995 (1968).
[12] S. Gorodetzky, P. Mennrath, W. Benenson, P. Chevallier, F. Scheibling, and G. Sutter, Phys. Letters **2**, 43 (1962).

TABLE II. 1p-1h wave functions for the $T=1$ 1^- and 2^- levels of mass 16. The origin of the wave functions is given in Table I.

N^{16} State	Calc.	$p_{1/2}^{-1}2s_{1/2}$ $C_{1/2,1/2}$	$p_{1/2}^{-1}d_{5/2}$ $C_{1/2,5/2}$	$p_{1/2}^{-1}d_{3/2}$ $C_{1/2,3/2}$	$p_{3/2}^{-1}2s_{1/2}$ $C_{3/2,1/2}$	$p_{3/2}^{-1}d_{5/2}$ $C_{3/2,5/2}$	$p_{3/2}^{-1}d_{3/2}$ $C_{3/2,3/2}$
1^-	jj	1.00	...	...	...	...	...
	EF	0.98	...	0.01	−0.16	−0.08	−0.02
	GJ	0.995	...	−0.008	0.026	−0.096	−0.020
	KLS	0.986	...	0.017	−0.053	−0.149	−0.038
2^-	jj	...	1.00	...	...	...	...
	EF	...	0.98	−0.10	0.06	0.14	0.09
	GJ	...	0.983	0.007	0.054	0.174	0.035
	KLS	...	0.960	−0.021	0.093	0.252	0.076

of the mass 16 $T=1$ odd-parity states and the O^{16} $(J^\pi,T)=(0^+,0)$ states.

The comparison between experiment and the nuclear model calculations is most easily done through the β moment, i.e., the square of the β-decay matrix element. The first step in extracting the β moment from the experimental partial half-lives is to calculate the ft values for the various β-ray branches. We have done this for the unique first-forbidden decays to the O^{16} ground state and 6.05-MeV level. The half-life for β^- decay of N^{16} is 7.37 ± 0.04 sec[13] while the branching fractions to the O^{16} ground state and 6.05-MeV level are 0.26 ± 0.02 and $(1.2\pm0.4)\times10^{-4}$, respectively; thus the respective partial half-lives are 28 ± 2 and $(6.1\pm2.0)\times10^4$ sec. The calculation of f_1, the statistical rate factor appropriate for unique first-forbidden decay, is discussed in the Appendix. Using β^- endpoint energies[14] of 10.422 ±0.0035 and 4.370 ± 0.004 MeV for the O^{16} ground state and 6.05-MeV level, respectively, we find f_1 values of 4.676×10^7 and 1.558×10^5; thus

$$f_1t|_{g.s.}=(1.33\pm0.10)\times10^9 \text{ sec},$$
$$f_1t|_{6.05}=(9.57\pm3.2)\times10^9 \text{ sec},$$

or

$$\log f_1t|_{g.s.}=9.12\pm0.04,$$
$$\log f_1t|_{6.05}=9.98\pm0.15.$$

These f_1t values correspond to β moments of [see Eq. (A26)]

$$\langle G_1\rangle_{g.s.}{}^2=1.49\pm0.12F^2,$$
$$\langle G_1\rangle_{6.05}{}^2=0.21\pm0.07F^2,$$

so that

$$\langle G_1\rangle_{6.05}{}^2/\langle G_1\rangle_{g.s.}{}^2=f_1t|_{g.s.}/f_1t|_{6.05}=0.14\pm0.05.$$

The latter result is quite different than a previous limit ($<1/30$) given for this ratio.[1,10] The reason for this is not that the present measurement differs greatly from the previous limit[1] but that the previous ratio was calculated using f_0t, appropriate for allowed β transitions, rather than f_1t as used here.

Comparison of the experimental values for $\langle G_1\rangle_{g.s.}{}^2$ and $\langle G_1\rangle_{6.05}{}^2$ with various nuclear model predictions is given in Table I. All the calculations considered which give a wave function for the $J^\pi=2^-$ N^{16} ground state also give one for the lowest $(J^\pi,T)=(1^-,1)$ state of O^{16}. Thus we include in Table I a comparison of experiment and theory for $E1$ transitions from the 13.09-MeV level of O^{16} (which is identified with the lowest J^π, $T=1^-$, 1 state of O^{16}). In this way the probability of accidental agreement of theory and experiment is decreased. The $E1$ transition strength, $\Lambda(E1)$, is defined by

$$\Gamma_\gamma(E1)=6.25\times10^{-2}E_\gamma{}^3\Lambda(E1)\ eV,$$

with E_γ in MeV. The theoretical expression used to calculate the $E1$ results of Table I is

$$\Lambda(E1)=(4/9)\gamma^{-1}\alpha^2[C_{1/2,1/2}+(\sqrt{5})C_{1/2,3/2}+\sqrt{2}C_{3/2,1/2}+3C_{3/2,5/2}-C_{3/2,3/2}]^2, \quad (2)$$

where the $C_{j_hj_p}$ are the expansion amplitudes for a one-particle–one-hole (1p-1h) wave function including the $p_{3/2}$, $p_{1/2}$, $2s_{1/2}$, $d_{5/2}$, and $d_{3/2}$ shells. The sign convention appropriate to Eq. (2) is (i) all radial wave functions positive at the origin, and (ii) either $\mathbf{s}+\mathbf{l}=\mathbf{j}$ with $\mathbf{j}_h+\mathbf{j}_p=\mathbf{J}$ or $\mathbf{l}+\mathbf{s}=\mathbf{j}$ with $\mathbf{j}_p+\mathbf{j}_h=\mathbf{J}$. In Eq. (2), $\gamma^{-1/2}$ is the radial falloff parameter of harmonic-oscillator wave functions, which we take to be 1.68 F. Equation (2) gives the $E1$ rate for that part of the $E1$ matrix element which connects a 1p-1h wave function with the closed shell s^4p^{12}, and α is the amplitude of s^4p^{12} in the O^{16} 0^+ state in question. The analogous expression for the β moment, $\langle G_1\rangle^2$, is given by multiplying Eq. (A25) by α^2. In Table I we give theoretical results for four different sets of 1p-1h wave functions. The $C_{j_hj_p}$ used in these calculations are listed in Table II.

In the top of Table I we have used $\alpha=1.0$ for the O^{16} ground state and 0.0 for the 6.05-MeV level. These, then, are the results for a model in which the O^{16} ground state and 6.05-MeV level are the ideal spherical and ideal deformed 0^+ states, the assumption being that the latter does not connect to a 1p-1h state. In the middle of Table I we give results for a model in which the ideal spherical and ideal deformed states

[13] F. Ajzenberg-Selove and T. Lauritsen, Nucl. Phys. **11**, 1 (1959).

[14] The endpoint energy for the ground-state transition is calculated from the mass tables of J. H. E. Mattauch, W. Thiele, and A. H. Wapstra, Nucl. Phys. **67**, 1 (1965). The endpoint energy for the transition to the 6.05-Mev level involves the ground-state endpoint energy and an excitation energy of 6.052 ± 0.002 MeV for this level. This value was obtained from an excitation energy of 6131.22 ± 0.46 keV for the O^{16} second excited state [C. Chasman, K. W. Jones, R. A. Ristinen, and D. E. Alburger, Phys. Rev. **159**, 830 (1967)] and a separation energy of 79 ± 2 keV between the 6.05- and 6.13-MeV levels (see Ref. 8 and the text).

are mixed:

$$\Psi(\text{g.s.})=\alpha\Psi_{\text{spher}}+\beta\Psi_{\text{def}},$$
$$\Psi(6.05\text{-MeV level})=\beta\Psi_{\text{spher}}-\alpha\Psi_{\text{def}}, \quad (3)$$

so that $\Lambda(E1)_{\text{g.s.}}$ and $\langle G_1\rangle_{\text{g.s.}}^2$ are reduced by α^2 and $\Lambda(E1)_{6.05}/\Lambda(E1)_{\text{g.s.}}=\langle G_1\rangle_{6.05}^2/\langle G_1\rangle_{\text{g.s.}}^2=\beta^2/\alpha^2$. We have used $\alpha=0.874$ and $\beta=-0.262$ in these calculations. Actually these are the expansion amplitudes α_0 and α_1 of Brown and Green,[15] who assumed

$$\Psi_i(0^+)=\alpha_i\Psi(\text{0p-0h})+\beta_i\Psi(\text{2p-2h})+\gamma_i\Psi(\text{4p-4h}). \quad (4)$$

Therefore, the results given in the middle of Table I are appropriate also to a model which combines the 1p-1h wave function with the Brown-Green wave functions for the 0^+ states with the additional assumption that the contributions to the matrix elements from 1p-1h $\rightarrow$ 2p-2h transitions are negligible. We will discuss this latter assumption further, but first we consider the results of Table I.

We see from Table II that for all three shell-model calculations considered[16–18] the $T=1$ 1^- and 2^- levels are nearly pure jj coupling states. Nevertheless, the small departures from jj coupling are important in the $E1$ and β^- matrix elements. This is shown by the reductions from the jj value of $\Lambda(E1)_{\text{g.s.}}$ and $\langle G_1\rangle_{\text{g.s.}}^2$ in all three cases. It is well known that the reduction of the $E1$ strength is associated with enhancement of the $E1$ strength in the highest two 1p-1h 1^- states (the $E1$ giant resonance). The reduction of $\langle G_1\rangle^2$, or of $\Lambda(M2)$, which is for practical purposes the same thing (see Sec. 3 of the Appendix), is quite analogous, and is associated with an enhancement of $\langle G_1\rangle^2$ for the highest two 1p-1h 2^- states.

We now ask if a model of mixed spherical and deformed states can explain simultaneously the $E1$ and β^- rates. We see from Table I that all three sets of 1p-1h wave functions give rather satisfactory agreement with the ground-state matrix elements; however, for no set is the agreement for both $\Lambda(E1)_{\text{g.s.}}$ and $\langle G_1\rangle_{\text{g.s.}}^2$ perfect. More importantly, we see that our model cannot give simultaneous agreement of $\Lambda(E1)_{6.05}/\Lambda(E1)_{\text{g.s.}}$ and $\langle G_1\rangle_{6.05}^2/\langle G_1\rangle_{\text{g.s.}}^2$ since experimentally they differ by a factor of ~ 3, while our model predicts them to be the same. We are led then to consider refinements to the model. We consider next the 1p-1h $\rightarrow$ 2p-2h contributions to the matrix elements. Since the $T=1$ 1^- and 2^- 1p-1h states are practically pure $p_{1/2}^{-1}2s_{1/2}$ and $p_{1/2}^{-1}d_{5/2}$, the important parts of the 1p-1h $\rightarrow$ 2p-2h $E1$ and β^- matrix elements are those which connect to $p_{1/2}^{-2}2s_{1/2}^2$ and $p_{1/2}^{-2}d_{5/2}^2$, respectively. The ratio of these contributions relative to the 1p-1h $\rightarrow$ 0p-0h contributions is given by Eq. (A22) for both the $E1$ and β^- transitions. It is found that these contributions are intrinsically small. In order to evaluate these small terms it is necessary to estimate the $\alpha(J_0,T_0)$ coefficients of Eq. (A22). Thus we leave the Brown-Green O^{16} wave functions and take up ones which give very similar values for the α_i, β_i, γ_i of Eq. (4), but which give the 2p-2h wave functions explicitly. These are provided by the recent shell-model calculations of Zuker *et al.*,[19] whose wave functions for the O^{16} 0^+ states can be put in the form of Eq. (4). This procedure is inconsistent—since in the calculations of Zuker *et al.* the $p_{3/2}$ shell is inert and the $T=1$ states are 1p-1h+3p-3h and we neglect the 3p-3h part—but gives plausible wave functions adequate for a first estimate. The results obtained from these wave functions are shown in the bottom of Table I. It is found that the inclusion of the 1p-1h $\rightarrow$ 2p-2h contributions changes the two ratios of transition strengths to the O^{16} 6.05-MeV level and ground state in the right direction. The logical next step would appear to be inclusion of the 3p-3h admixtures in the odd-parity states. Actually the calculations of Zuker *et al.*[19] indicate that such admixtures are quite strong.

ACKNOWLEDGMENTS

We would like to thank R. Jaffe and Professor G. E. Brown of Princeton University, who guided us in our considerations of the theoretical predictions of the $E1$ and β^- transition rates. B. Buck and A. Zuker provided us with preliminary results of their shell-model wave functions and advised us in their use.

APPENDIX: UNIQUE n-FORBIDDEN β DECAY

1. Connection Between β Moment and Comparative Half-Life

We define the β moment $\langle G_n\rangle^2$ for unique n-forbidden β decay with $n=0$, 1, 2, etc., by[20–22]

$$\langle G_n\rangle^2=\frac{(\ln 2)(2\pi^3/g^2C_A^2)([(2n+1)!!]^2/(2n+1))\lambda\!\!\!^{-}_{ce}{}^{2n}}{f_nt}, \quad (A1)$$

where f_nt is the comparative half-life and $\lambda\!\!\!^{-}_{ce}$ is the Compton wavelength of the electron. Giving f_nt and $(\ln 2)(2\pi^3/g^2C_A^2)$ the units of time, $\langle G_n\rangle^2$ has the units of $\lambda\!\!\!^{-}_{ce}{}^{2n}$.

Equation (A1) holds for $|J_i-J_f|=n+1$ and $\pi_i\pi_f=(-)^n$; however higher moments can enter unless either J_i or J_f is equal to 0, in which case $\langle G_n\rangle^2$ is the only β moment which can connect the states J_i and J_f.

[15] G. E. Brown and A. M. Green, Nucl. Phys. **75**, 401 (1966).
[16] J. P. Elliott and B. H. Flowers, Proc. Phys. Soc. (London) **A242**, 57 (1957).
[17] V. Gillet and D. A. Jenkins, Phys. Rev. **140**, B36 (1965).
[18] S. Kahana, H. C. Lee, and C. K. Scott (private communication).
[19] A. P. Zuker, B. Buck, and J. B. McGrory, Phys. Rev. Letters **21**, 39 (1968).
[20] The treatment given here follows closely from that of Refs. 21 and 22.
[21] E. J. Konopinski, *The Theory of Beta Radioactivity* (Oxford University Press, Oxford, England, 1966).
[22] E. J. Konopinski and M. E. Rose, in *Alpha-, Beta-, and Gamma-Ray Spectroscopy*, edited by K. Siegbahn (North-Holland Publishing Co., Amsterdam, 1965), Vol. II, p. 1327.

The statistical rate factor can be expressed as[21,22]

$$f_n=\int_1^{W_0} a_n(Z)F(Z,W)pW(W_0-W)^2dW, \quad \text{(A2)}$$

where W is the β energy and W_0 is the disintegration energy both in units of the electron rest mass (and including the rest mass), $F(Z,W)$ is the ratio of the electron density at the nucleus to the density at infinity, and $a_n(Z)$ is the shape factor. We have included Coulomb effects and nuclear size effects in our calculation of $F(Z,W)$ and $a_n(Z)$. This was done to order $(\alpha Z)^2$ using a nuclear radius of $1.2A^{1/3}$ F. It was found that Coulomb effects were not significant for $Z\approx 8$: We might as well have assumed $Z=0$ in our calculation of $a_n(Z)$. This approximation, valid for $|Z/137|^2\ll 1$, gives,[21,22] in our normalization,

$$a_n(0)=(2n+1)!\sum_{\nu=0}^{n}(W^2-1)^\nu(W_0-W)^{2(n-\nu)}/(2\nu+1)!(2n-2\nu+1)!, \quad \text{(A3)}$$

in particular $a_1(0)=(W^2-1)+(W_0-W)^2$. Note that $a_0(Z)\equiv 1$. The statistical rate factor f_n was evaluated by numerical integration of Eq. (A2).

2. Evaluation of β Moment

The β moment is defined theoretically by

$$\langle G_n\rangle^2=\frac{1}{(2J_i+1)}\sum_{M_iM_fm}|\langle J_fM_f|G_n{}^m|J_iM_i\rangle|^2=\frac{\langle J_f\|G_n\|J_i\rangle^2}{(2J_i+1)}, \quad \text{(A4)}$$

where the definition of the Wigner-Eckart theorem follows de Shalit and Talmi[23] and the matrix element on the right is reduced with respect to **J**. If an isospin formalism is used we have

$$G_n=\sum_{j=1}^{A}\frac{1}{\sqrt{2}}\tau_q{}^{(j)}r_j{}^n[\mathbf{C}^{(n)}\times\boldsymbol{\sigma}]_j{}^{(n+1)}, \quad \text{(A5)}$$

where the sum is over the A nucleons of the nucleus, τ_q is a component of the spherical isospin tensor,

$$\tau_q=-\tfrac{1}{2}\sqrt{2}q(\tau_x+iq\tau_y), \quad \tau_0=\tau_z, \quad \text{(A6)}$$

and $q=\pm 1$ for $\beta^\pm$ decay. The tensor $\mathbf{C}_n$ is an unnormalized surface harmonic tensor, i.e.,

$$\mathbf{C}_m{}^{(n)}(\hat{r})=[4\pi/(2n+1)]^{1/2}\mathbf{Y}_{nm}(\hat{r}). \quad \text{(A7)}$$

Thus, we have

$$\langle G_n\rangle=(-)^{T_i-T_f-q}\frac{(T_fT_{zf}1-q|T_iT_{zi})}{[2(2T_i+1)]^{1/2}}\times\frac{|\langle J_fT_f\|\sum_{j=1}^{A}\tau^{(j)}r_j{}^n[\mathbf{C}^{(n)}\times\boldsymbol{\sigma}]_j{}^{(n+1)}\|J_iT_i\rangle|}{(2J_i+1)^{1/2}}, \quad \text{(A8)}$$

where $T_z=\frac{1}{2}(N-Z)$, $(T_fT_{zf}1-q|T_iT_{zi})$ is a vector-addition coefficient, and the matrix element on the right is now reduced with respect to both **J** and **T**. The m component of the $(n+1)$-rank irreducible tensor $[\mathbf{C}^{(n)}\times\boldsymbol{\sigma}]^{(n+1)}$ is defined by the tensor product[23]

$$[\mathbf{C}_n(\hat{r})\times\boldsymbol{\sigma}]_m{}^{(n+1)}=\sum_\mu(nm-\mu 1\mu|n+1m)C_{m-\mu}{}^{(n)}(\hat{r})\sigma_\mu. \quad \text{(A9)}$$

Or, in terms of the vector spherical harmonics defined by[22]

$$\mathbf{T}_{Jm}{}^L(\hat{r})=\sum_{\mu=0,\pm1}(Lm-\mu 1\mu|Jm)Y_{L,m-\mu}(\hat{r})e_\mu, \quad \text{(A10)}$$

where $\mathbf{e}$ is a unit vector, we have[24]

$$[C_n(\hat{r})\times\boldsymbol{\sigma}]_m{}^{(n+1)}=[4\pi/(2n+1)]^{1/2}T_{n+1,m}{}^n(\hat{r})\cdot\boldsymbol{\sigma}. \quad \text{(A11)}$$

The same operator [Eq. (A11)] appears in the matrix elements of ML γ-ray transitions but usually appears in the form on the left of Eq. (A12)[23,25]:

$$\text{grad}[r^LC_M{}^{(L)}]\cdot\boldsymbol{\sigma}=[L(2L-1)]^{1/2}r^{L-1}[\mathbf{C}^{(L-1)}\times\boldsymbol{\sigma}]_M{}^{(L)}. \quad \text{(A12)}$$

3. Connection Between γ and β Matrix Elements

The connection between unique n-forbidden β decay and ML γ emission, where $L=n+1$, can be obtained from Eq. (A12). We write the transition strength for a $\Delta T=1$ ML γ-ray transition in the form[26]

$$\Lambda(ML)=[\lambda(ML)]^2=[\lambda_j(ML)+\lambda_j(ML)]^2, \quad \text{(A13)}$$

where we have separated the contributions to $\lambda(ML)$ using $\mathbf{j}=\mathbf{l}+\frac{1}{2}\boldsymbol{\sigma}$. The γ-decay matrix element is given by

$$\lambda(ML)=\frac{\langle J_f\|H(ML)\|J_i\rangle}{(2J_i+1)^{1/2}}, \quad \text{(A14)}$$

where

$$H(ML)=\frac{1}{2}\left(\mu_- -\frac{1}{L+1}\right)\sum_{i=1}^{A}\tau_0{}^{(i)}\,\text{grad}[r^LC_M{}^{(L)}]_i\cdot\boldsymbol{\sigma}^{(i)}+\frac{1}{L+1}\sum_{i=1}^{A}\tau_0{}^{(i)}\,\text{grad}[r^LC_M{}^{(L)}]_i\cdot\mathbf{j}^{(i)}, \quad \text{(A15)}$$

with $\mu_-=\mu_p-\mu_n=4.71$ in units of nuclear magnetons. From Eqs. (A8), (A12), and (A15) we can write the following relationship between the β and γ (spin part) matrix elements connecting the T_i, T_{zf} (γ decay) and T_i, $T_{zf}-q$ (β decay) members of the $(2T_i+1)$ set of

[23] A. deShalit and I. Talmi, *Nuclear Shell Theory* (Academic Press Inc., New York, 1963).

[24] In Refs. 21 and 22 the β moment is written as $\langle\boldsymbol{\sigma}\cdot\mathbf{T}_n{}^{(n+1)}\rangle^2$. In a similar shorthand notation our moment is $[4\pi/(2n+1)]\langle r^n\mathbf{T}_n{}^{(n+1)}\cdot\boldsymbol{\sigma}\rangle^2$.

[25] E. K. Warburton and W. T. Pinkston, Phys. Rev. **118**, 733 (1960).

[26] The transition strength is defined in magnitude by Eqs. (A6) and (A7) of Ref. 25.

analog states to a common T_f, T_{zf} final state:

$$\lambda_\sigma(ML)=\frac{1}{\sqrt{2}}\left(\mu_- -\frac{1}{L+1}\right)\frac{(T_fT_{zf}1\quad 0|T_iT_{zf})}{(T_fT_{zf}1-q|T_iT_{zf}-q)}\times[L(2L-1)]^{1/2}\langle G_{L-1}\rangle. \quad \text{(A16)}$$

On the average we expect $\lambda_\sigma(ML)$ to dominate $\lambda_j(ML)$ simply because μ_- is large compared to unity (for a single-particle transition with $|j_i-j_f|=L$ λ_j is zero). Thus we expect $\Lambda(ML)\approx[\lambda_\sigma(ML)]^2$ for transitions of average or greater than average strength. This relationship, Eq. (A16), is well known for allowed ($n=0$) Gamow-Teller β decay. We see that it can be extended to all n-forbidden unique β decay.[27]

4. β Moments for Simple Models

We now consider the evaluation of Eq. (A4) for a single-particle (s.p.) transition $l_is_ij_i\to l_fs_fj_f$. In this case Eq. (A8) gives[23]

$$\langle G_n\rangle_{\text{s.p.}}=6^{1/2}(2n+3)^{1/2}(2j_f+1)^{1/2}\langle r^n\rangle_{l_il_f}\times\langle l_f\|\mathbf{C}^{(n)}\|l_i\rangle\begin{Bmatrix} l_f & \frac{1}{2} & j_f\\ l_i & \frac{1}{2} & j_i\\ n & 1 & n+1\end{Bmatrix}, \quad \text{(A17)}$$

where a $9j$ coefficient appears on the far right.[28] $\langle r^n\rangle_{l_il_f}$ stands for $\langle l_f\|r^n\|l_i\rangle$, and

$$\langle l_f\|\mathbf{C}^{(n)}\|l_i\rangle=(-)^n(2l_f+1)^{1/2}(l_f0n0|l_i0).$$

If $l_i=l_f+n$, $j_i=j_f+n+1$, e.g., $d_{5/2}\to p_{1/2}$, $f_{7/2}\to d_{3/2}$, etc., for $n=1$, then Eq. (A17) reduces to[21]

$$(2j_f+1)^{-1/2}\langle G_n\rangle_{\text{s.p.}}=2^{1/2}\frac{(2n!)^{1/2}}{n!}\left(\frac{(2j_f+1)!}{(2j_i)!}\right)^{1/2}\frac{(j_i-1/2)!}{(j_f+1/2)!}\langle r^n\rangle_{l_il_f}. \quad \text{(A18)}$$

Equation (A18) also gives $\langle G_n\rangle$ for

$$l_f=l_i+n,\quad j_f=j_i+n+1,$$

if j_i and j_f are interchanged on the right.

The expression for $\langle G_n\rangle$ which pertains for a transition from a 1p-1h state to a closed shell (vacuum), i.e., $j_h^{-1}j_p)_{J_i}\to j_h^0)_{0+}$ is quite simply

$$\langle G_n\rangle_{\text{1p-1h}}=\left[\frac{(2j_p+1)}{(2J_i+1)}\right]^{1/2}\langle G_n\rangle_{\text{s.p.}}, \quad \text{(A19)}$$

where the right side is to be evaluated from Eq. (A17) for $j_i=j_p$, $j_f=j_h$.

A $(J_iT_i)=(J_i,1)$ 1p-1h state, $j_h^{-1}j_p$, is also connected to a $(J_f,T_f)=(0,0)$ 2p-2h state by $\langle G_n\rangle$. We give the connection to that part of the 2p-2h wave function given by

$$\sum_{J_0,T_0}\alpha(J_0,T_0)\Psi[(j_h^{-2})_{J_0,T_0}(j_p^2)_{J_0,T_0}]_{0,0}, \quad \text{(A20)}$$

with (J_0,T_0) restricted to (0,1) or (1,0). This matrix element we designated by $\langle G_n\rangle_{\text{2p-2h}}$. It is given by

$$\langle G_n\rangle_{\text{2p-2h}}=S(J_i)\langle G_n\rangle_{\text{1p-1h}}, \quad \text{(A21)}$$

where

$$S(J_i)=\frac{(-)^{J_i+1}}{[3(2j_h+1)(2j_p+1)]^{1/2}}\left[\alpha(0,1)-\frac{6[j_h(j_h+1)+j_p(j_p+1)-J_i(J_i+1)]}{[2j_h(2j_h+2)2j_p(2j_p+2)]^{1/2}}\alpha(1,0)\right]. \quad \text{(A22)}$$

For example, a $J_i=2^-$, $p_{1/2}^{-1}d_{5/2}\to p_{1/2}^{-2}d_{5/2}^2$ transition gives

$$S(2)=\frac{-1}{6}[\alpha(0,1)-(\sqrt{21}/5)\alpha(1,0)]. \quad \text{(A23)}$$

5. $N^{16}{}_{g.s.}\to O^{16}{}_{g.s.}$ β Moment

If we take

$$\Psi(J_i^\pi=2^-,T=1)=C_{1/2,5/2}\Psi(p_{1/2}^{-1}d_{5/2})+C_{1/2,3/2}\Psi(p_{1/2}^{-1}d_{3/2})+C_{3/2,1/2}\Psi(p_{3/2}^{-1}2s_{1/2})+C_{3/2,5/2}\Psi(p_{3/2}^{-1}d_{5/2})+C_{3/2,3/2}\Psi(p_{3/2}^{-1}d_{3/2}) \quad \text{(A24)}$$

for the wave function of the N^{16} ground state and the doubly closed s^4p^{12} configuration for the O^{16} 0^+ final state, we obtain from Eqs. (A17), (A19), and (A24),[29]

$$\langle G_1\rangle^2=(8/5)\gamma^{-1}[C_{1/2,5/2}+0.204C_{1/2,3/2}-0.645C_{3/2,1/2}-0.935C_{3/2,5/2}-0.408C_{3/2,3/2}]^2. \quad \text{(A25)}$$

We have used harmonic-oscillator radial wave functions to evaluate $\langle r\rangle_{l_il_f}$ with the result $\langle r\rangle_{pd}=(\sqrt{\frac{5}{2}})\gamma^{-1/2}$, $\langle r\rangle_{ps}=-\gamma^{1/2}$, where γ is the radial falloff parameter in F. In application of Eq. (A25) we have used $\gamma^{-1/2}=1.68$ F.

The experimental values of $\langle G_1\rangle^2$ were obtained from Eq. (A1) using experimental values of ft,

$$(\ln 2)(2\pi^3/g^2C_A^2)\simeq 4.4\times10^3 \text{ sec} \quad \text{(Refs. 21, 22)}$$

and $\lambda\!\!\!^{-}_{ce}=386.1$ F, i.e.,

$$\langle G_1\rangle_{\text{expt}}^2=\frac{19.68\times10^8}{(f_1t)_{\text{expt}}}\text{ F}^2. \quad \text{(A26)}$$

[27] This connection has previously been discussed by A. Bohr and B. R. Mottelson, Kgl. Danske Videnskab Selskab, Mat. Fys. Medd. **27**, No. 16 (1953).

[28] The $9j$ coefficient of Eq. (A17) can be expressed in terms of $6j$ coefficients as follows:

$$\begin{Bmatrix} lf & \frac{1}{2} & j_f\\ l_i & \frac{1}{2} & j_i\\ n & 1 & n+1\end{Bmatrix}=-\tfrac{1}{3}\begin{Bmatrix} j_f & j_i & n+1\\ \frac{1}{2} & n+\frac{1}{2} & l_i\end{Bmatrix}\begin{Bmatrix} l_i & l_f & n\\ \frac{1}{2} & n+\frac{1}{2} & j_f\end{Bmatrix}\Big/\begin{Bmatrix} n+1 & n & 1\\ \frac{1}{2} & \frac{1}{2} & n+\frac{1}{2}\end{Bmatrix}.$$

[29] Three phase conventions are pertinent to Eqs. (A23) and (A25). These are $\mathbf{j}_h+\mathbf{j}_p=\mathbf{J}_i$ with $\mathbf{s}+\mathbf{l}=\mathbf{j}$ or $\mathbf{j}_p+\mathbf{j}_h=\mathbf{J}_i$ with $\mathbf{l}+\mathbf{s}=\mathbf{j}$, and the $2s$ harmonic-oscillator wave function is positive at the origin.